Defect and Diffusion Forum Vols. 297-301 (2010) pp 330-337
Online available since 2010/Apr/13 at www.scientific.net

doi:10.4028/www.scientific.net/DDF.297-301.330

Thermal Properties and Crystallization Behavior of *Co*67*Fe*4*Cr*7*Si*8*B*14 Amorphous Alloy

M. Haddad-Sabzevar[1], S. Sahebian, Z. Jamili, S.A. Hasheminejad

Department of Metallurgy and Materials Engineering, Engineering Faculty, Ferdowsi University of Mashhad, Azadi Square, Mashhad, Iran

[1]haddadm@ferdowsi.um.ac.ir

Keywords: crystallization kinetics, Co amorphous alloy, DSC.

Abstract. In order to investigate the crystallization behavior of the *Co*67*Fe*4*Cr*7*Si*8*B*14 amorphous metallic alloy, ribbons of this alloy were prepared by planar flow melt spinning process (PFMS). Differential scanning calorimetery (DSC) and differential thermal analyzer (DTA) were used to analyze the thermal properties and crystallization behavior of the samples at three heating rates of 10, 20 and 30 ºC/min. The experimental data were fitted to the Avrami model to determine the crystallization behavior. The results showed that the crystallization exotherm became wider and shifted toward a higher temperature range as the heating rate increased. The Avrami analysis also showed that n is about 1, which is related to the same transformation mechanism at different heating rates. The Kissinger method was used to determine the activation energy for the first crystallization peaks. The measured value is approximately 332.67 kJ/g.

Introduction

The first amorphous metallic alloy was produced in the Au-Si system by a rapid solidification technique. This class of materials is characterized by the lack of long-rang order in their structure [1, 2]. Several methods are used to prepare the amorphous materials, in the forms of ribbon or wire. They are based on rapid cooling of liquid metals and alloys, or condensing their vapor on a cold substrate, as well as some other methods [3, 4]. All these methods render amorphous materials with excellent chemical, electrical, mechanical and magnetic properties. Metallic amorphous alloys are in a metastable state, so they can crystallize when heated or held at high temperature for sufficient time. The physical properties, such as dimensional stability, heat capacity, electrical resistivity, volume and magnetic properties can change during the crystallization process [5-9].

Co- based crystalline alloys are widely used as magnetic materials. Alloys of the binary Co-B system can easily be amorphized by melt spinning. More complex alloys with specific properties can be obtained by addition of other elements to this system [10-11]. Various chemical compounds can be crystallized from the amorphous phase at some specific temperatures as well. Lesz *et al.* [9] investigated the crystallization behavior of $Co_{80}Si_9B_{11}$ using various methods. They showed that the α-Co phase was formed after annealing it at high temperatures. For higher annealing temperatures, the Co_3B and Co_2Si phases were formed. These phases decrease the relative magnetic permeability [9]. The crystallization behavior of the $Co_{65}Si_{15}B_{14}Fe_4Ni_2$ metallic glass was studied using DSC, resistivity, XRD and TEM by Li and Ramanujan [12] at high temperatures. The resistivity decreased sharply at 540, 630 and 750ºC. The first two resistivity drops correspond to the phases formed as α- Co, ε-Co, Co_2Si, Co_3B in the first and Co_2B, Co_4B in the second crystallization stages respectively.
The crystallization of materials is usually studied by the DSC method. The crystallization process can proceed under either isotherm or non-isothermal conditions. From a practical point of view, the non isothermal crystallization is the dominant mode of crystallization. Little attention has been

given to the crystallization behavior of a Co amorphous alloy. The aim of this research is to find out the effect of thermal treatment on the crystallization kinetics of the mentioned amorphous alloys using a DSC analyzer.

Experimental Procedure

The alloy used for this study was *Co*67*Fe*4*Cr*7*Si*8*B*14. The test alloy was prepared from pure materials and melted in a vacuum furnace. The planar flow melt spinning (PFMS) process was used for producing continuous ribbons [13]. The samples were remelted in an induction furnace, using a quartz tube with an inner diameter of about 20 mm serving as a crucible under argon atmosphere. The crucible had a rectangular nozzle measuring 0.4×20 mm for producing amorphous ribbons. The distance between the wheel and the nozzle was held between 0.25-0.35 mm. 12-15g of alloys were melted in each run reaching a linear speed of 25 m/s. A Pt- Pt-10%Rd thermocouple was positioned inside the melt to control its temperature. The melt was ejected by blowing argon at different casting temperatures. From this alloy, continuous ribbons of about 20 mm width were produced, using a 290 mm in diameter copper wheel as a substrate.
In order to observe the microstructure of the amorphous ribbon using optical microscope, the sample was etched by V2A solution for about 5 minutes.
The amorphous structure of the Co ribbon was determined by X-ray diffraction (XRD, D8 Advance with Cu-Kα radiation). Prior to XRD experiment the sample was heated to 400°C at a heating rate of 10ºC/min, and held at 400°C for 30 minutes in an Argon atmosphere. An XRD measurement was recorded on the solid sample in the form of a ribbon.
A Shimadzu DSC60 differential scanning calorimeter (DSC) was used to study the crystallization behavior of Co amorphous alloy. The temperature scale was calibrated by pure indium standard (T_m=156.6°C and ΔH_f = 28.5 J/g) in every run to ensure accuracy and reliability of the data. The analyzed samples having a mass of about 2 mg were placed in an Al pan, with an empty pan used as a reference. The crystallization kinetics of the Co amorphous ribbon was determined by continuous heating in a DSC at heating rates of 10, 20 and 30 ºC/min.
Due to the limitation on working temperature of our DSC analyzer, DTA analysis (NETZSCH 404) was used to determine the crystallization temperatures at above the capability of DSC analyzer. The mass of the sample was about 0.2 gram. To determine the crystallization temperature, the sample was heated to 1000 K at a heating rate of 10ºC/min.

Results and discussion

Figure 1 shows the optical micrographs of Co amorphous sample after etching. This sample does not show any microstructure related to the amorphous state. In addition to optically study to check the amorphous structure of Co alloy, X-ray diffraction was used. Before the XRD test, the sample was annealed at 673 K and held for 30 minutes at this temperature. The diffraction pattern of Co sample as a function of 2θ is shown in figure 2. Based on this figure, the X-ray diffraction pattern without any sharp peak is detected in this study, which indicates that the *Co*67*Fe*4*Cr*7*Si*8*B*14 sample keeps its amorphous state after annealing.
In order to define the thermal characteristics of amorphous ribbon, the kinetics of crystallization during heating using thermal analysis is usually investigated [14]. In this way, different heating rates are applied to the material and one property is measured proportionally connected with the degree of conversion (crystallization) versus time and temperature.

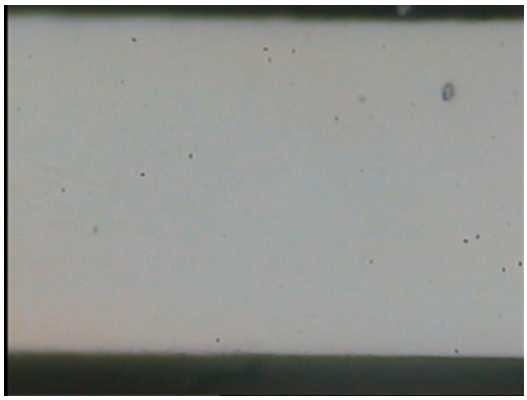

Figure 1. Optical micrograph for Co amorphous alloy (1000x).

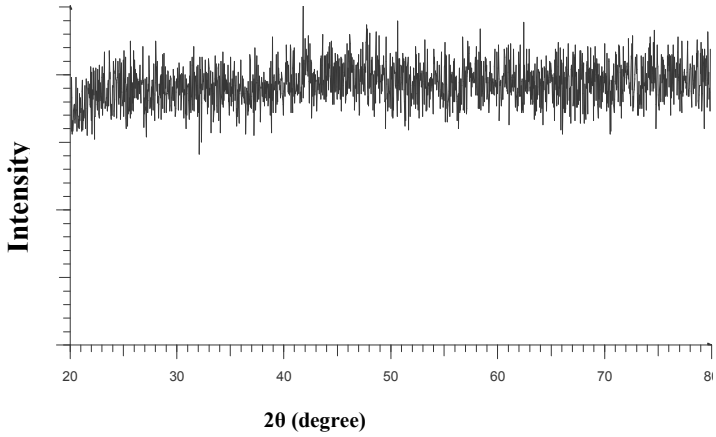

Figure 2. X-ray diffraction pattern of the Co amorphous alloy after annealing at 400 ° C for 30 min.

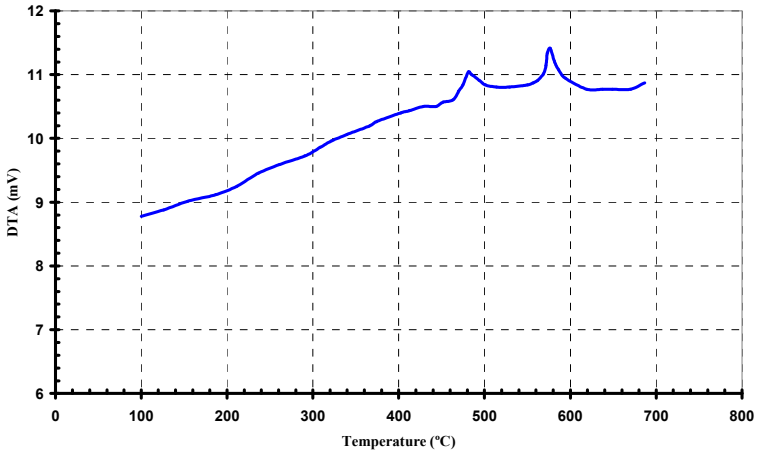

Figure 3. DTA curve of amorphous *Co*67*Fe*4*Cr*7*Si*8*B*14 alloy at a heating rate of 10°C/min.

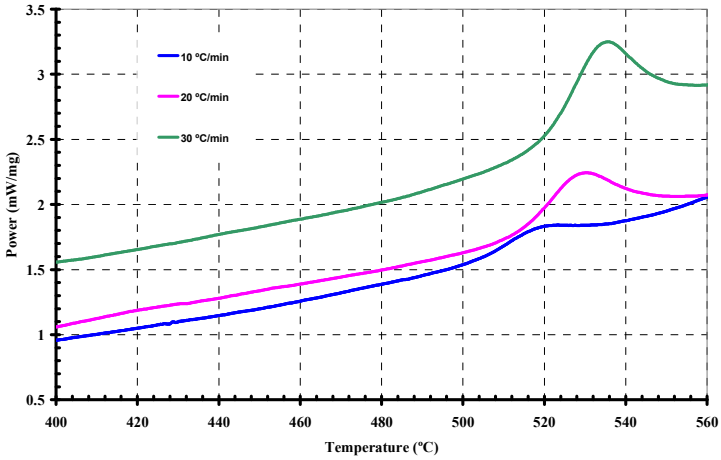

Figure 4. DSC thermo grams of non-isothermal crystallization at different cooling rate for the Co amorphous alloy.

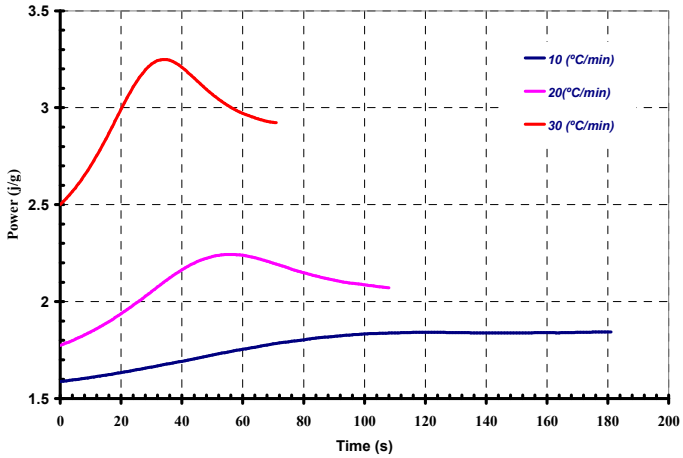

Figure 5. Power as a function of time of the Co amorphous alloy at different cooling rates ranging from 10 to 30 ºC/min.

Figure 3 shows the non-isothermal DTA curve for *Co*67*Fe*4*Cr*7*Si*8*B*14 alloy at a heating rate of $10\ ^{\circ}C/_{\min}$. As can be seen in Figure (3), the crystallization process occurs at two stages due to two exothermic peaks at about $T_1 = 517^{\circ}$ C and $T_2 = 600^{\circ}$ C, respectively.

Figures 4 and 5 show the non-isothermal heating DSC plots for the Co amorphous ribbon at different heating rates of 10, 20 and 30º C/min. As seen from these figures, the crystallization of the amorphous *Co*67*Fe*4*Cr*7*Si*8*B*14 alloy occurred in one stage up to 550° C. It was also observed that when the heating rate increases, the crystallization peak become wider and shifts toward the higher temperature.

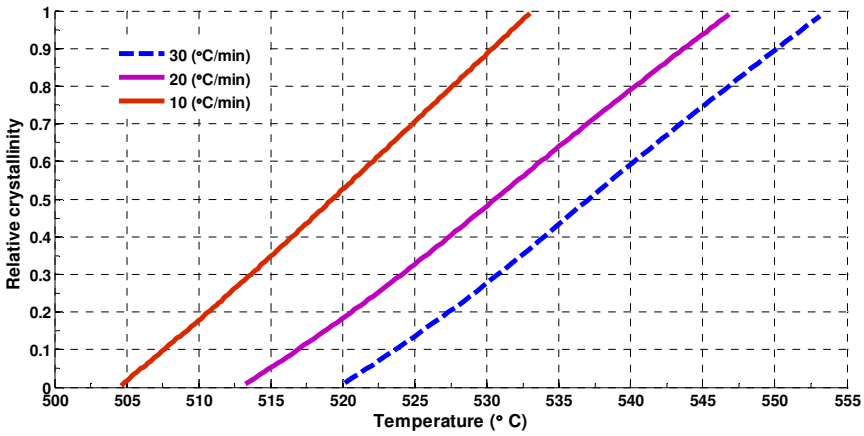

Figure 6. Relative crystallinity index as a function of temperature of the Co amorphous alloy at different cooling rates ranging from 10 to 30 ºC/min.

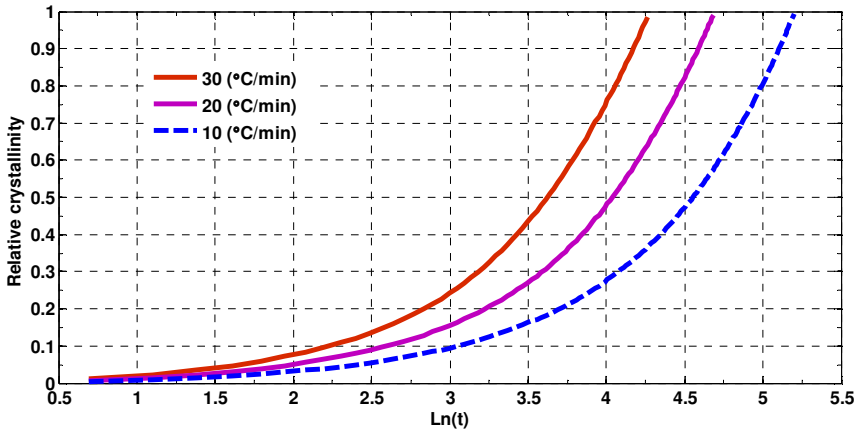

Figure 7. Plots of relative crystallinity as a function of time for the Co amorphous alloy crystallized non-isothermally at various cooling rates.

Integration of the exothermic peak during the non-isothermal crystallization gave the relative degree of crystallinity as a function of temperature, which is easily transformed to the plot of relative crystallinity vs. time at different heating rates. By using the DSC test, the energy released over the non-isothermal crystallization process as a function of temperature could be obtained. As a result, the relative crystallinity index as a function of time and temperature could be defined as [15]:

$$X(t) = \frac{\int_{T_0}^{T} \left(\frac{dH}{dT}\right) \times dT}{\int_{T_0}^{T_\infty} \left(\frac{dH}{dT}\right) \times dT} \qquad (1)$$

where X(t), T_0 and T_∞ are the relative crystallinity index, the onset and endset crystallization temperature, respectively, and $\left(\frac{dH}{dT}\right)$ is the heat flow rate. T is the crystallization temperature at time t. The relative crystallinity index as a function of temperature and time for Co amorphous alloy at various cooling rates are illustrated in Figures 6 and 7, respectively. According to Figure 7, it is

clear that the faster heating rate leads to a shorter required time for the completion of the crystallization process.

Based on the exotherm peaks of Figures 6 and 7, some quantitative data, such as the temperature at 1% relative crystallinity $T_{0.01}$, temperature at the maximum crystallinity T_P, temperature at 99% relative crystallinity $T_{0.99}$, and heat of crystallization could be obtained. These results are summarized in Table I. It is clear that these values shift toward a higher temperature value with increasing heating rate.
The non-isothermal crystallization data analyzed based on the Avrami model, Equations 2 and 3 can be arranged to the following form [16-18].

$$X(t) = 1 - \exp(-(kt)^n) \quad (2)$$

$$\ln[-\ln(1 - X_t)] = n \times \ln(k) + n \ln(t) \quad (3)$$

where K and n are the Avrami rate constant and the Avrami exponent, respectively. Based on these equations, the Avrami kinetic parameters (i.e. k,n) could be obtained from the plot of $\ln[-\ln(1 - X_t)]$ vs. ln(t), as shown in Figure 8. The slope of the straight line is n, and the intercept is ln k. Table II summarizes the values of the Avrami kinetic parameters along with the values of the r^2 parameter signifying the quality of the fitting during the crystallization process. Based on the values of the r^2 parameter, it can be concluded that the Avrami model is suitable for describing the non-isothermal crystallization data of the sample at various heating rates. Based on data in Table II, The Avrami exponent is seen to be independent of the heating rate, and the value of n for Co amorphous alloy is about 1.

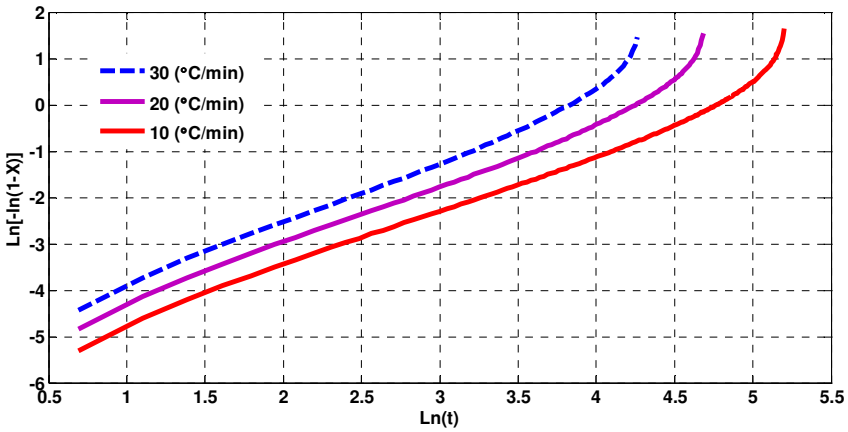

Figure 8. Plots of the variation of $\ln[-\ln(1 - X_t)]$ versus ln(t) for the Co amorphous alloy at various cooling rate.

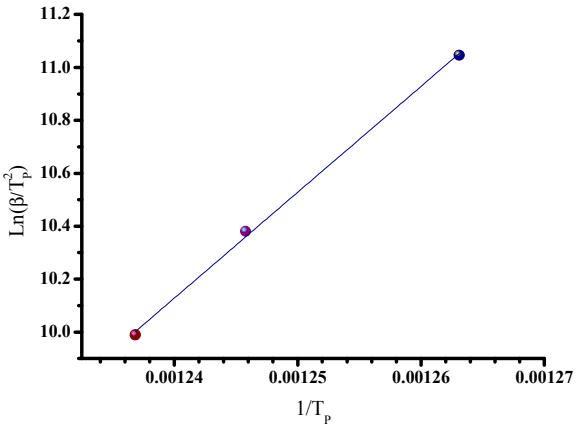

Figure 9. Kissinger plot of the variation of $\ln\left(\frac{\phi}{T_P^{\,2}}\right)$ versus $\frac{1}{T_P}$ for the Co amorphous alloy.

Table I: Characteristic data of exotherm peak after non-isothermal crystallization for Co amorphous alloy.

Φ (°C/min)	$T_{0.01}$ (°C)	T_P (°C)	$T_{0.99}$ (°C)	ΔH (jg^{-1})
10	504.1	518.7	533.1	16.82
20	512.6	529.7	546.6	29.54
30	519.1	535.5	553.2	35.75

Table II: Non- isothermal crystallization kinetics for Co amorphous alloy based on avrami analysis for crystallization process.

Φ (°C/min)	Ln(k)	n	r^2
10	-5.77	1.162	0.9995
20	-5.41	1.22	0.9997
30	-5.1	1.282	0.9995

The activation energy ΔE can be determined using the Kissinger approach [19] by calculating the variation of T_p with the heating rate ϕ by the following relation:

$$\frac{d\ln\left(\frac{\phi}{T_P^{\,2}}\right)}{d\left(\frac{1}{T_P}\right)} = \frac{-\Delta E}{R} \qquad (4)$$

where R is the gas constant, ϕ, T_p and ΔE are the heating rate, peak of temperature and activation energy, respectively. The activation energy can be calculated from the slopes of $\ln\left(\frac{\phi}{T_P^{\,2}}\right)$ vs. $\frac{1}{T_P}$ (Figure 9). The activation energy of Co amorphous alloy equals to 332.67 kJ/g, and the R-squared value is 0.99779.

Conclusion

The amorphous *Co*67*Fe*4*Cr*7*Si*8*B*14 ribbon keeps its amorphous structure up to near 500°C and over this temperature, structural changes of the Co alloy initiates as seen peak in DSC plot. The crystallization of the amorphous *Co*67*Fe*4*Cr*7*Si*8*B*14 alloy occurs in two stages. With increasing heating rate, the crystallization peak becomes wider and shifts to a high temperature.
The Avrami model is suitable for describing non-isothermal crystallization data of the sample at various heating rates. The Avrami exponent is independent of the heating rate, and the value of n for the Co amorphous alloy is about 1. Also, the activation energy is determined as 332.67 kj/g by the means of the Kissinger analysis.

References

1. J.D. Bernal: Nature Vol. 185 (1960), p. 68.
2. S. Takayma: J. Mat. Sci. Vol. 11 (1976), p. 164.
3. P. Duwez, R.H. Willens, Klement: J. Appl. Phys. Vol. 31 (1960), p. 1136.
4. N.J.Grant and B.C.Gissen (Eds.), *Rapidly Quenched Metals*, MIT Press, 1976.
5. M.G. Scott, in: F.E. Luborsky (Ed.), *Amorphous Metallic Alloys*, Butterworths, London, 1983, p.144.
6. Z.Zh. Yuan, X-D. Chen, H.Xu, X-L. Qu and B-X Wang: J. Alloys Comps. Vol. 422 (2006), p. 109.
7. S-W Hwang, D-H. Im, I.S.Chun, C.S.Yoon and C.K. Kim: J. Alloys Comps. Vol. 413 (2006), p.206.
8. S. Murty, B. Kotur, L. Bednarska, Yu. Kulyk, A. Korolyshyn, O. Hertsyk: J. Alloys Comps. Vol. 367 (2004), p. 274.
9. S. Lesz, R. Nowosielski, A. Zajdel, B. Kostrubiec and Z. Stoklosa: Intern. Sci. Journal Vol. 28 (2007), p. 91.
10. H. Beck and H.J. Guntherodt (Eds.) *Glassy Metals II, Atomic Structure and Dynamics, Electronic Structure, Magnetic Properties*, Springer, 1983.
11. S.R. Nagel, J. Tauc : Sol. St. Commun. Vol. 22 (1977), p. 129.
12. H.F. Li and R.V. Ramanujan: Mat. Sci. and Eng. A Vol. 375-377 (2004), p. 1087.
13. M. Haddad-sabzevar, Doctoral Thesis, *Ribbon Formation and Solidification Behavior in Planar Flow Melt Spinning Process*, Royal Institute of Technology S-100 44 Stockholm, , Dept. of Materials Processing, October 1994.
14. S.D. Kalushkin and I.A. Tomilin, Thermochim: Acta. Vols. 280-281 (1996), p. 303.
15. M. Joshi and B. S. Butala: Polymer Vol. 45 (2004), p. 4953.
16. M. Avrami : J. Chem. Phys. Vol. 7 (1939), p. 1103.
17. M. Avrami : J. Chem. Phys. Vol. 8 (1940), p. 212.
18. M. Avrami : J. Chem. Physics. Vol. 9 (1941), p. 177.
19. H. E. Kissinger: J. Res. Nat. Bur. Standards (US) Vol. 57 (1956), p. 217.

Diffusion in Solids and Liquids V
doi:10.4028/www.scientific.net/DDF.297-301

Thermal Properties and Crystallization Behavior of Co67Fe4Cr7Si8B14 Amorphous Alloy
doi:10.4028/www.scientific.net/DDF.297-301.330

References

1. J.D. Bernal: Nature Vol. 185 (1960), p. 68.
doi:10.1038/185068a0
Can't connect to PubMed

2. S. Takayma: J. Mat. Sci. Vol. 11 (1976), p. 164.
doi:10.1007/BF00541088
Can't connect to PubMed

3. P. Duwez, R.H. Willens, Klement: J. Appl. Phys. Vol. 31 (1960), p. 1136.
doi:10.1063/1.1735777
Can't connect to PubMed

4. N.J.Grant and B.C.Gissen (Eds.), Rapidly Quenched Metals, MIT Press, 1976.
Can't connect to PubMed

5. M.G. Scott, in: F.E. Luborsky (Ed.), Amorphous Metallic Alloys, Butterworths, London, 1983, p.144.
Can't connect to PubMed

6. Z.Zh. Yuan, X-D. Chen, H.Xu, X-L. Qu and B-X Wang: J. Alloys Comps. Vol. 422 (2006), p. 109.
Can't connect to PubMed

7. S-W Hwang, D-H. Im, I.S.Chun, C.S.Yoon and C.K. Kim: J. Alloys Comps. Vol. 413 (2006), p.206.
doi:10.1016/j.jallcom.2005.03.113
Can't connect to PubMed

8. S. Murty, B. Kotur, L. Bednarska, Yu. Kulyk, A. Korolyshyn, O. Hertsyk: J. Alloys Comps. Vol. 367 (2004), p. 274.
doi:10.1016/j.jallcom.2003.08.055
Can't connect to PubMed

9. S. Lesz, R. Nowosielski, A. Zajdel, B. Kostrubiec and Z. Stoklosa: Intern. Sci. Journal Vol. 28 (2007), p. 91.
Can't connect to PubMed

10. H. Beck and H.J. Guntherodt (Eds.) Glassy Metals II, Atomic Structure and Dynamics,

Electronic Structure, Magnetic Properties, Springer, 1983.
Can't connect to PubMed

11. S.R. Nagel, J. Tauc : Sol. St. Commun. Vol. 22 (1977), p. 129.
doi:10.1016/0038-1098(77)90417-3
Can't connect to PubMed

12. H.F. Li and R.V. Ramanujan: Mat. Sci. and Eng. A Vol. 375-377 (2004), p. 1087.
doi:10.1016/j.msea.2003.10.109
Can't connect to PubMed

13. M. Haddad-sabzevar, Doctoral Thesis, Ribbon Formation and Solidification Behavior in Planar Flow Melt Spinning Process, Royal Institute of Technology S-100 44 Stockholm, Dept. of Materials Processing, October 1994.

14. S.D. Kalushkin and I.A. Tomilin, Thermochim: Acta. Vols. 280-281 (1996), p. 303.
doi:10.1016/0040-6031(96)02926-7
Can't connect to PubMed

15. M. Joshi and B. S. Butala: Polymer Vol. 45 (2004), p. 4953.
doi:10.1016/j.polymer.2004.04.057
Can't connect to PubMed

16. M. Avrami : J. Chem. Phys. Vol. 7 (1939), p. 1103.
doi:10.1063/1.1750380
Can't connect to PubMed

17. M. Avrami : J. Chem. Phys. Vol. 8 (1940), p. 212.
doi:10.1063/1.1750631
Can't connect to PubMed

18. M. Avrami : J. Chem. Physics. Vol. 9 (1941), p. 177.
doi:10.1063/1.1750872
Can't connect to PubMed

19. H. E. Kissinger: J. Res. Nat. Bur. Standards (US) Vol. 57 (1956), p. 217.
Can't connect to PubMed